



THE NON-LINEAR ANALYSIS OF THE EFFECT OF SUPPORT CONSTRUCTION PROPERTIES ON THE DYNAMIC PROPERTIES OF MULTI-SUPPORT ROTOR SYSTEMS

J. KICIŃSKI, R. DROZDOWSKI AND P. MATERNY

*The Institute of Fluid-Flow Machinery, The Polish Academy of Sciences, Fiszerza 14,
80-952 Gdańsk, Poland*

(Received 11 October 1996, and in final form 15 May 1997)

The paper reports on the course of simulation research of large rotor machines (200 MW power turbine sets) carried out at the Institute of Fluid-Flow Machinery, Polish Academy of Sciences (IFFM PAS). The investigations draw on a non-linear theoretical model and a developed computer code. The paper presents the main assumptions of this model and examples of its experimental verification. An attempt is made to classify the hydrodynamic instability of the system, in a diagnostic manner. The analysis of dynamic properties of a 200 MW turbo-set is concentrated on two selected problems, the first of which is the effect of thermoelastic deformation of the bearing bushes on the lateral forced vibration of the rotor line system. The simulation research is conducted on the basis of a three-dimensional elastodiathermal model of the bearing nodes. This enables the modelling of complex processes of heat transfer in the bearing, as well as the validation of arbitrary methods of fixing and action areas of the initial clamping forces. The second problem is the analysis, based on the finite element method, of dynamic properties of the LP casing at the fixing points of the bearing bushes.

© 1997 Academic Press Limited

1. NON-LINEAR MODELS IN ROTOR DYNAMICS OF TURBO-MACHINERY

The modelling of dynamics of real rotor lines and turbo-set supports is a very complex problem. One can distinguish some characteristic substructures, each of which is a separate problem: journal bearings; labyrinth seals; rotor supports with bearing external fixings; foundations; rotor lines with discs, clutches and other rotating elements. The first three have non-linear characteristics. In particular, the characteristics of journal bearings are highly non-linear. These problems have been the subjects of investigations by many authors [1–8]. Usually, the authors of these works have assumed a simple model of the journal bearings. However, the problems which are connected with the heat transfer in the bearing, especially during large displacements of a journal in the area of the oil gap, are neglected in the non-linear analysis of this simple model. At IFFM PAS in Gdańsk, a complex non-linear model of large rotor machines, as well as a series of computer programs, have been worked out in order to conduct simulation research on large turbo-sets.

Journal bearings are the most difficult substructure to be theoretically modelled. The stiffness and damping features of the oil film are described by four stiffness coefficients $c_{i,k}$ and four damping coefficients $d_{i,k}$, shown in Figure 1(a). With a large displacement of the journal, the coefficients $c_{i,k}$ and $d_{i,k}$ depend on the journal location e , γ and the displacement

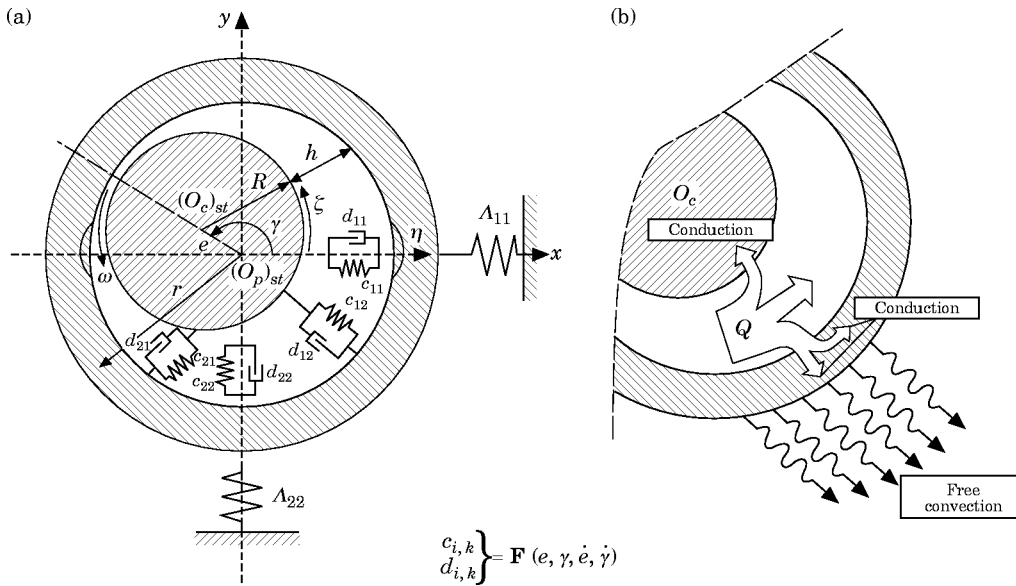


Figure 1. The diagram of viscous-elastic characteristics of the oil film (a) and the model of heat exchange in the bearing (b).

speed \dot{e} , $\dot{\gamma}$, so they vary in time in a highly non-linear way (a list of nomenclature is given in the Appendix).

In what follows, a new approach to the problem is suggested in which the stiffness and damping coefficients are defined by means of a perturbation analysis of the modified disturbing differential equations. The equations are integrated simultaneously with the Reynolds equation within the common boundaries ξ_1^* and ξ_2^* .

The boundaries ξ_1^* and ξ_2^* are the origin and end of the continuous oil film area, and thereby the end and origin of the cavitation zone. The same boundaries ξ_1^* and ξ_2^* then define the hydrodynamic pressure distribution and disturbing functions, from which the film stiffness and damping coefficients are calculated. The modification of the perturbation analysis is based on the reduction from four to two in the number of disturbing equations solved simultaneously with the Reynolds equation, which greatly improves the calculation speed. The above-mentioned reduction in the number of disturbing equations is possible under the assumption that the disturbing functions $\partial p/\partial x$, $\partial p/\partial y$, $\partial p/\partial \dot{x}$, and $\partial p/\partial \dot{y}$ are equal to zero at the boundaries of the integration area. This assumption is usually valid for journal bearings. It is possible to prove that applying the divergence theorem (Gauss–Ostrogradsky) to the disturbing equations enables one to obtain eight values of the stiffness and damping coefficients by integration of only the two disturbing equations for $\partial p/\partial \dot{x}$ and $\partial p/\partial \dot{y}$.

The procedures and mathematical proofs connected with the reduction in the number of disturbing equations can be found in reference [9]. The integration limits for the Reynolds equation and disturbing equations are not constant in time. Generally, they should be written as $\xi_1^*(t)$ and $\xi_2^*(t)$. ξ_1^* and ξ_2^* are defined by the condition of oil-flow continuity within the oil clearance, which involves the evaluation of the boundary of the cavitation zone and considering the so-called “flow prehistory”, in which time is not a parameter but an independent variable. The relevant information is available in references [10, 11]. The magnitudes demanded of the stiffness coefficients $c_{i,k}$ and damping coefficients $d_{i,k}$ are evaluated by integrating the functions $\partial p/\partial x$ and $\partial p/\partial y$.

Another problem is the definition of the average “effective” oil viscosity that appears in the dynamic equations. In the model presented, the viscosity for the conditions of kinetostatic load of the bearing is defined by means of an elastodiathermal heat model. This model describes the 3-D heat transfer by means of convection and conduction, and is based on the 3-D Reynolds equation, energy and conduction equations, as well as 3-D equations for deformation of the oil gap (see Figure 1(b)). The elastodiathermal model of the heat transfer was presented in references [12, 13]. When the coefficients $c_{i,k}$ and $d_{i,k}$ for the journal bearings and the coefficients for the labyrinth seals are known, it is possible to define in a similar way and introduce conceivably non-linear characteristics of the bearing external fixings evaluated by integrating the functions $\partial p/\partial \dot{x}$ and $\partial p/\partial \dot{y}$. Using the finite element method (FEM), one can model the stiffness and damping interactions between the oil film, labyrinth seal and bearing external fixings (by means of point finite elements—PFE), rotor elements (using the definition of substitute diameters for the moments of inertia), rotating mass (by means of beam finite elements—BFE) and discs (by means of stiff finite elements).

As a result, one obtains a general equation of motion in the form.

$$\mathbf{M}\ddot{\mathbf{q}} + \mathbf{D}(\mathbf{q}, \dot{\mathbf{q}}, \mathbf{t})\dot{\mathbf{q}} + \mathbf{K}(\mathbf{q}, \dot{\mathbf{q}}, \mathbf{t})\mathbf{q} = \mathbf{P}(\mathbf{t}), \quad (1)$$

where \mathbf{M} is the global inertia matrix of the system, \mathbf{D} is the global damping matrix which contains coefficients of damping of the rotor material, oil film, bush external fixing and labyrinth seals, \mathbf{K} is the global stiffness matrix which contains stiffness coefficients as above, \mathbf{q} is the displacement vector and \mathbf{P} is the vector of the excitation force, arbitrary and non-linearly time-variable—for example, asynchronous electric excitation of the generator or forces caused by clutch misalignment.

The algorithm suggested separates the kinetostatic part (the definition of the reactions of bearing external fixings, thermal calculations of the bearings and the evaluation of viscosity $\bar{\mu}$) and the dynamic part for which at every time step $t + \Delta t$ the conjugated dynamic equations are solved. Eventually, for a sufficiently small Δt and a sufficiently large number of iterations (for periodic dynamic loads), one obtains a converged solution. In the algorithm presented the equations of motion were integrated directly by means of Newmark’s method with coefficients $\alpha = \beta = 1/4$. In view of the character of the equations of motion (their strong non-linearity), Newmark’s method was modified by adding relaxation to the stiffness and damping coefficients of the oil film. The choice of relaxation coefficients was based on numerical tests. The conjunction of Newmark’s method with the relaxation method has not only significantly improved the stability of the numerical solution, but also enabled us to obtain solutions for a number of cases in which the other methods failed to converge at all. Based upon the above-mentioned algorithm, new computer programs KINWIR and NLDW have been developed. They allow advanced simulation research of large rotor machines.

In Figure 2 is presented the flowchart of the KINWIR and NLDW programs employed in the analysis of kinetostatics and dynamics problems in complex rotor/journal/bearing/support/foundation systems in the non-linear range.

For the sake of brevity, no presentation is given here of the basic equations of the model, such as the 3-D Reynolds equation, energy equation, conduction equation, continuity equation for the cavitation zone, as well as the perturbation equations used to define damping and elastic properties of the oil film, and the equations which define rotor and labyrinth seal models. The details concerning the construction of the global equations of motion (1), the discussion of the accepted assumptions and numerical integration of the equations will also not be presented here. The theoretical model and the computer programs were described in detail in reference [14]. The main purpose of this work is to

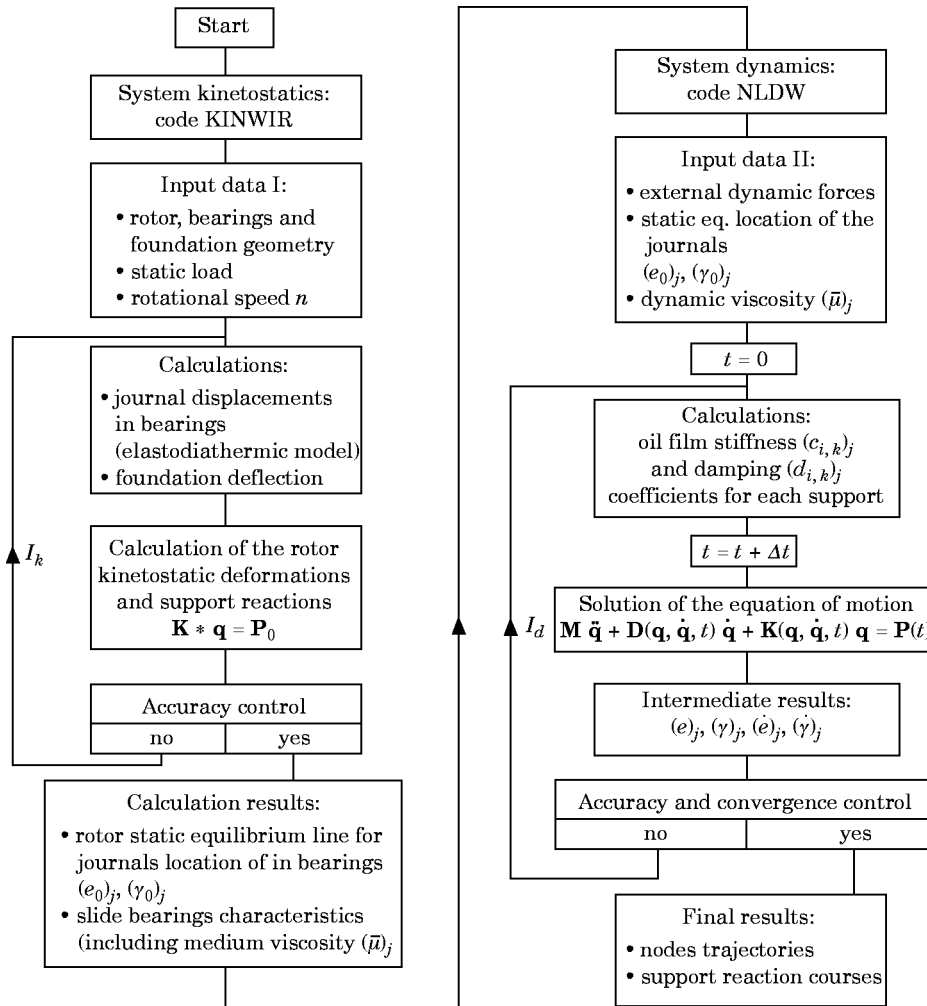


Figure 2. The flow chart of the KINWIR and NLDW programs.

give examples of experimental verification of the model and, primarily, to provide application examples of the created calculation tools for the simulation research of large rotor machines such as power turbo-sets.

However, to close this chapter, it is worth underlining the most characteristic and original features of the created model and computer programs.

(i) The non-linear description enables generation of the simulative vibration spectrum during the action of arbitrary external forces (asynchronous and time variable) and the evaluation of operation of the machine, also after exceeding the stability limit. This fact is very important in rotor machine diagnostics. Research becomes possible into such interesting phenomena as oil whirl or oil whip and general conditions for the occurrence of both large and small instabilities.

(ii) The kinetostatic and dynamic calculations of the system are possible, for an arbitrary shape of the bush centreline: i.e., during the misalignment of the rotor line or thermal displacement of the support during the operation. This creates a chance for

optimization calculations of the whole system being analyzed, including the thermal phenomena in journal bearings.

From a scientific aspect, the original features of this model are the following.

(i) The Reynolds equation and the disturbing equations, defining the stiffness and damping properties of the oil film, are integrated in common (and physically well-founded) boundaries ξ_1^* and ξ_2^* . These boundaries are defined on the basis of the flow continuity equation also in the cavitation zone.

(ii) The stiffness coefficients $c_{i,k}$ and damping coefficients $d_{i,k}$ of the bearing and labyrinth seals are defined by means of a modified perturbation method (reduction from four to two disturbing equations, which reduces the calculation time).

(iii) The average effective oil viscosity is defined, based on the complex elastodiathermal heat model of the bearing and thermoelastic deformation of the oil gap.

2. EXAMPLES OF EXPERIMENTAL VERIFICATION OF THE MODEL

The individual subsystems of the model, such as journal bearings or the rotor line, were verified on the basis of many years of experimental research conducted at IFFM PAS [9, 10]. To verify the complex model of the whole rotor/bearings/supports/foundation system, a large-size experimental rig was built; a diagram of this rig is presented in Figure 3. There is a five-support rotor with a total length of more than 6 m; the diameter of the shaft and the bearing journals is 0.1 m, and the diameter of the discs is 0.4 m. The distance between the supports is 1.4 m. Journal bearings of length/width ratio $L/D = 0.5$ and relative circular-cylindrical radial clearance $\Delta R/R = 0.0015-0.0018$ were used for the experiment. The discs unbalance corresponding to the displacement of their centres of mass, $\delta = 25 \times 10^{-6}$ m, was the excitation force. The experiment was conducted for two operating ranges: (I) the range of stable operation of the system—the experiment was performed for “stiff” external fixings of the bush ($\lambda_{11} = 0.9 \times 10^8$ N/m, $\lambda_{22} = 3 \times 10^8$ N/m);

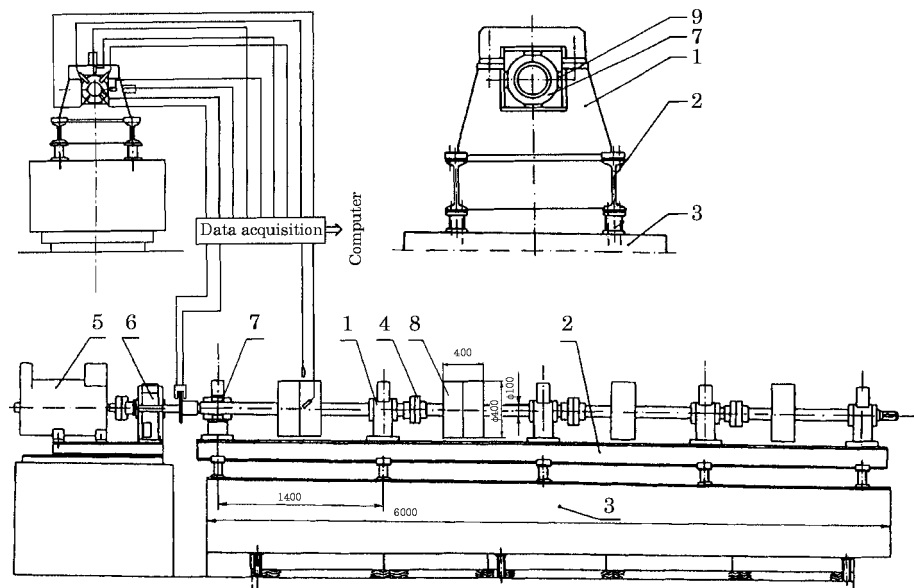


Figure 3. The construction sketch of a large-size rig for the investigation of dynamics of the rotor line; 1, supports; 2, foundation frame; 3, foundation; 4, clutches; 5, electric motor; 6, transmission; 7, slide bearings; 8, discs; 9, external fixings of the bushes.

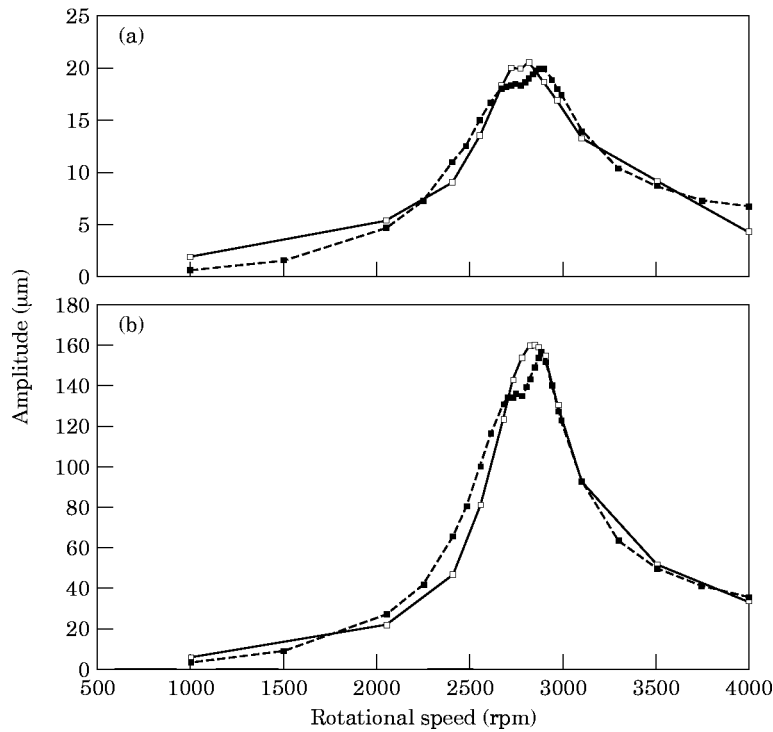


Figure 4. The theoretical (---■---) and experimental (—□—) vibration amplitudes for a selected journal (a) and disc centre (b).

(II) the range of small oil vibrations (oil whirls) for rotation velocities above the stability limit of the system—the experiment was conducted for “flexible” external fixings of the bush ($\lambda_{11} = 3 \times 10^6$ N/m, $\lambda_{22} = 6 \times 10^6$ N/m).

The results of the experiments are presented in Figures 4–7 (for the stable range) and in Figure 8 (for the unstable range).

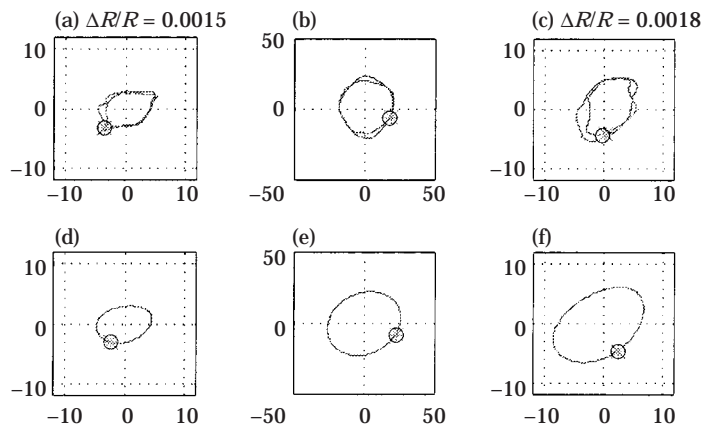


Figure 5. The comparison of measured (a–c) and calculated (d–f) trajectories for a pre-resonance rotational speed; $n = 2050$ rpm; scales in μm . (a), (c), (d), (f), Relative vibration of the journal for various radial clearances $\Delta R/R$; (b), (e), absolute vibration of the disc centre; \circ , the position marker of the excitation force vector for $t = 0^\circ$; $*$, the position marker of the excitation force vector for $t = 360^\circ$.

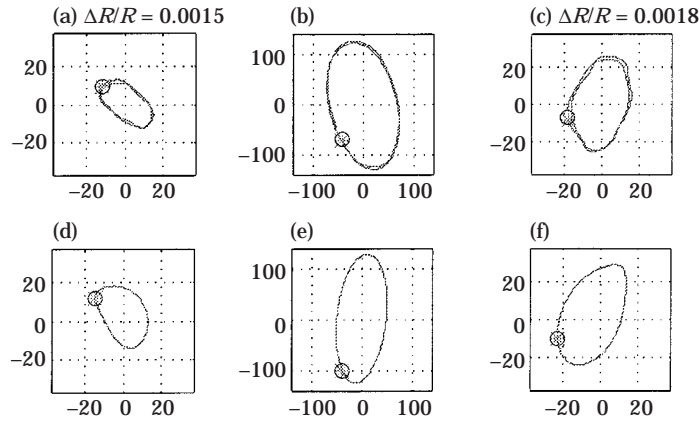


Figure 6. As Figure 5, but for an around resonance rotational speed of $n = 2972$ rpm.

On the basis of the results presented in Figures 4–7, it can be found that the consistency of the theoretical and experimental data is sufficiently satisfactory in the stable range, especially with respect to the amplitude values and the trajectory shape, as well as to the position markers of the exciting force vector (phase angles).

The example of verification of the model after exceeding the system stability limit, i.e., under the conditions of self-excited oil vibrations in the bearings, is presented in Figure 8. Here one observes the development of small oil whirls in the form of a characteristic half loop. The position markers of the exciting force vector for $\tau = 0^\circ$ and 360° (phase angles) undergo a “splitting”. At around $n = 3300\text{--}3350$ rpm, a sudden jump in the phase of the trajectory (see Figures 8(b) and (c)) and a lay down of the half-loop occur.

These phenomena of the half-loop development and the phase jumps were confirmed experimentally (see Figures 8(d)–(f)). A satisfying consistency of the vibration amplitudes and the phase-angle changes can be found here. The shapes of the trajectories differ slightly, which can be explained, first of all, by the mistakes in the accepted geometry of the bearing clearance (in comparison to the actual one).

It is worth mentioning here that the measurements of relative journal vibrations in bearings are particularly difficult. This difficulty occurs because of their size (from several to $20\ \mu\text{m}$) and the so-called “run-out” problem (the influence of material non-uniformity).

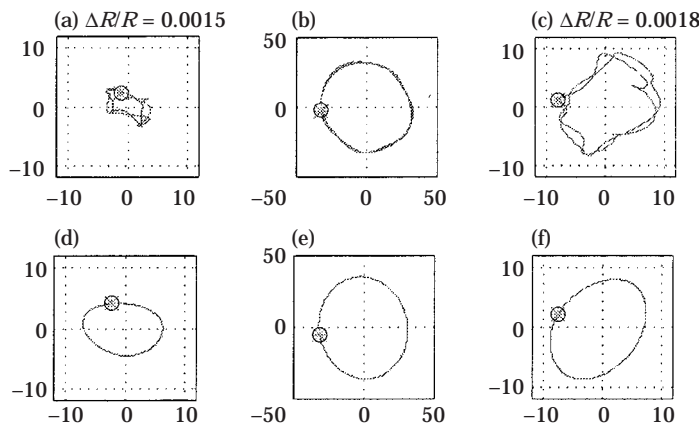


Figure 7. As Figure 5, but for a beyond-resonance rotational speed of $n = 4001$ rpm.

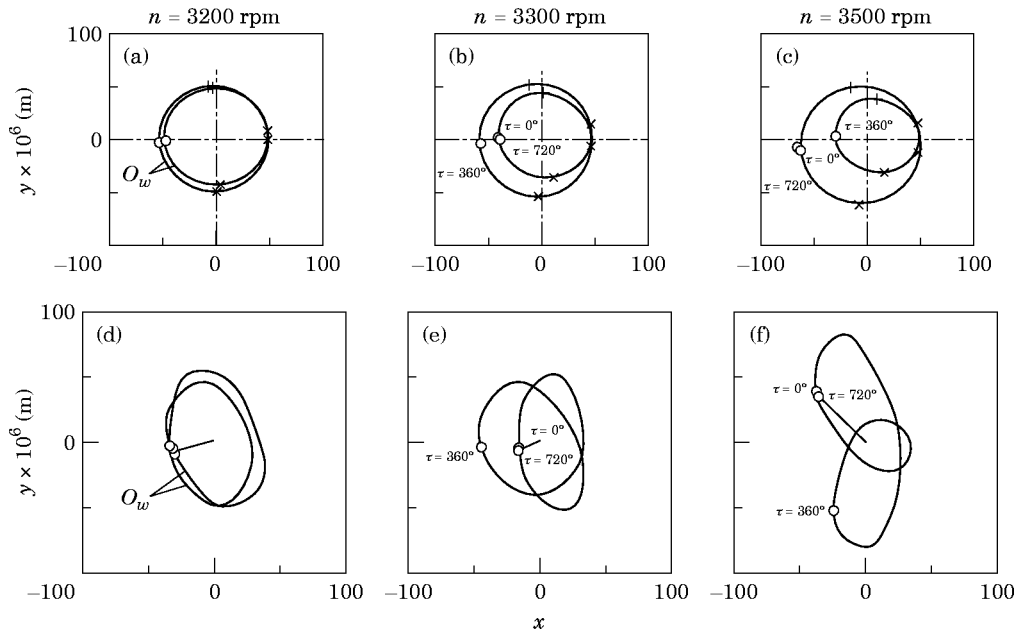


Figure 8. The verification of the model for the rotational speed range beyond the system stability limit. The development of small oil vibrations (oil whirls). The relative vibration of a selected journal. (a)–(c), Calculated trajectories; (d)–(f), measured trajectories; \circ , The position marker of the excitation force vector for $t = 0^\circ, 360^\circ$ and 720° .

For the needs of this verification, a special method has been created for a computer conditioning of the measuring signals, which come from the “run out”. In Figure 9 are presented a measured “raw” trajectory as well as a trajectory after computer conditioning.

The model verification research was also conducted for a series of other rotor speeds, other external forces and other stiffnesses of bush external fixing. In all cases analyzed the

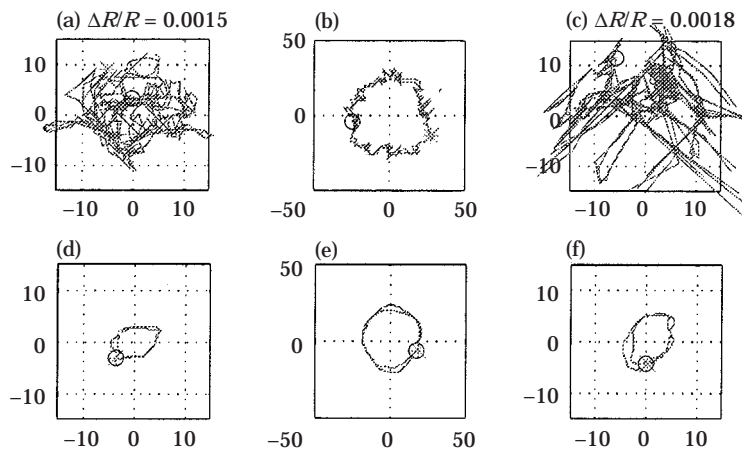


Figure 9. The effect of material non-uniformity (“run out”) on the results of measurements for a rotational speed $n = 2050$ rpm. (a)–(c) “Raw” trajectories; (d)–(f) results of computer “conditioning” of the signal. (a), (c), (d), (f), Trajectories of relative vibrations in the bearings; (b), (e), trajectories of absolute vibrations of the disc.

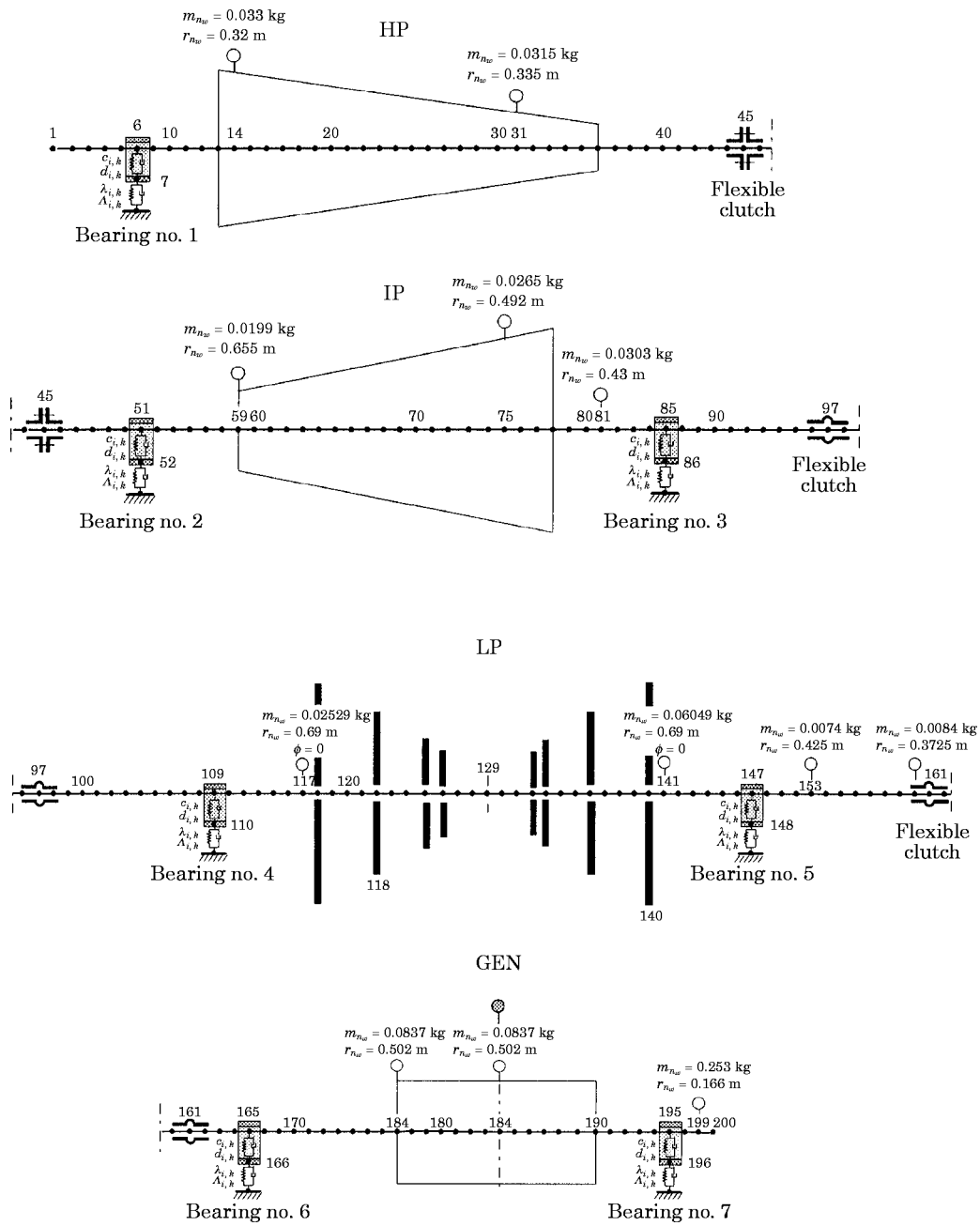


Figure 10. The diagram of FEM discretization of a 200 MW turbo-set.

consistency of the calculation results and measurements was satisfactory. The verification of the model is especially significant in the unstable strongly non-linear operating range. It confirms the usefulness of the model for the analysis of problems such as the instability of complex rotating systems over a wide range of rotational speeds.

3. EXAMPLES OF SIMULATION RESEARCH

3.1. THE EFFECT OF BUSH FIXING METHOD

In this section, the results of the simulation research of a large rotor machine, a 200 MW turbo-set are described. The FEM discretization of the rotor line of this machine together with the indicated accepted forces of the residual unbalance and the electric force in the generator, are presented in Figure 10.

Approaching the analysis of dynamic features of a large turbo-set by means of computer calculations, one faces a number of difficulties and restrictions connected with specifying some of the input data, even when equipped with such advanced simulation programs as the KINWIR and NLDW codes. These difficulties concern among others, such data as material and external damping coefficients, values of electric and steam forces influencing the system or defining the rotor unbalance vector in 3-D space.

One of the possible procedures in such cases is to estimate extreme values and to carry out parametric calculations, the prime aim of which is to disclose the tendencies for changing the characteristics and reveal the directions for the optimization of the system. The absolute level of vibration at a particular point will not be then as important as the sign of the change in the vibration amplitude or stability level of the trajectory as a function of, for instance, the shape of the kinetostatic line. This approach was applied in the calculation examples presented below.

One goal of the simulation research programme conducted at the Institute of Fluid-Flow Machinery of the Polish Academy of Science is to define the effect of the bush fixings in

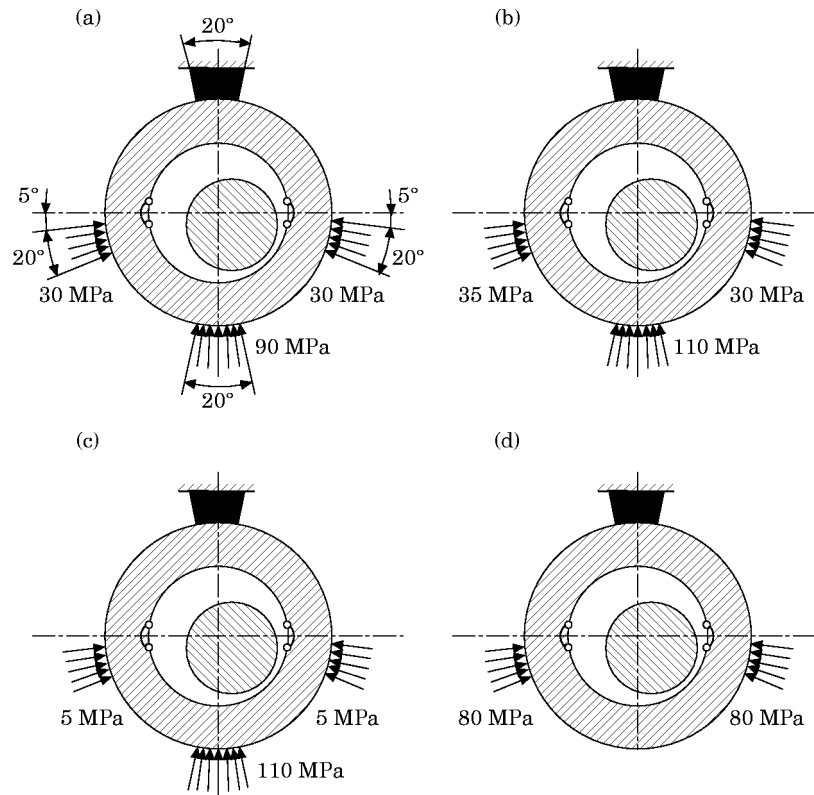


Figure 11. The load diagrams of bearing bush no. 6 under external forces—different versions of initial clamping, $n = 3000$ rpm. (a) case 1; (b) case 2; (c) case 3; (d) case 4.

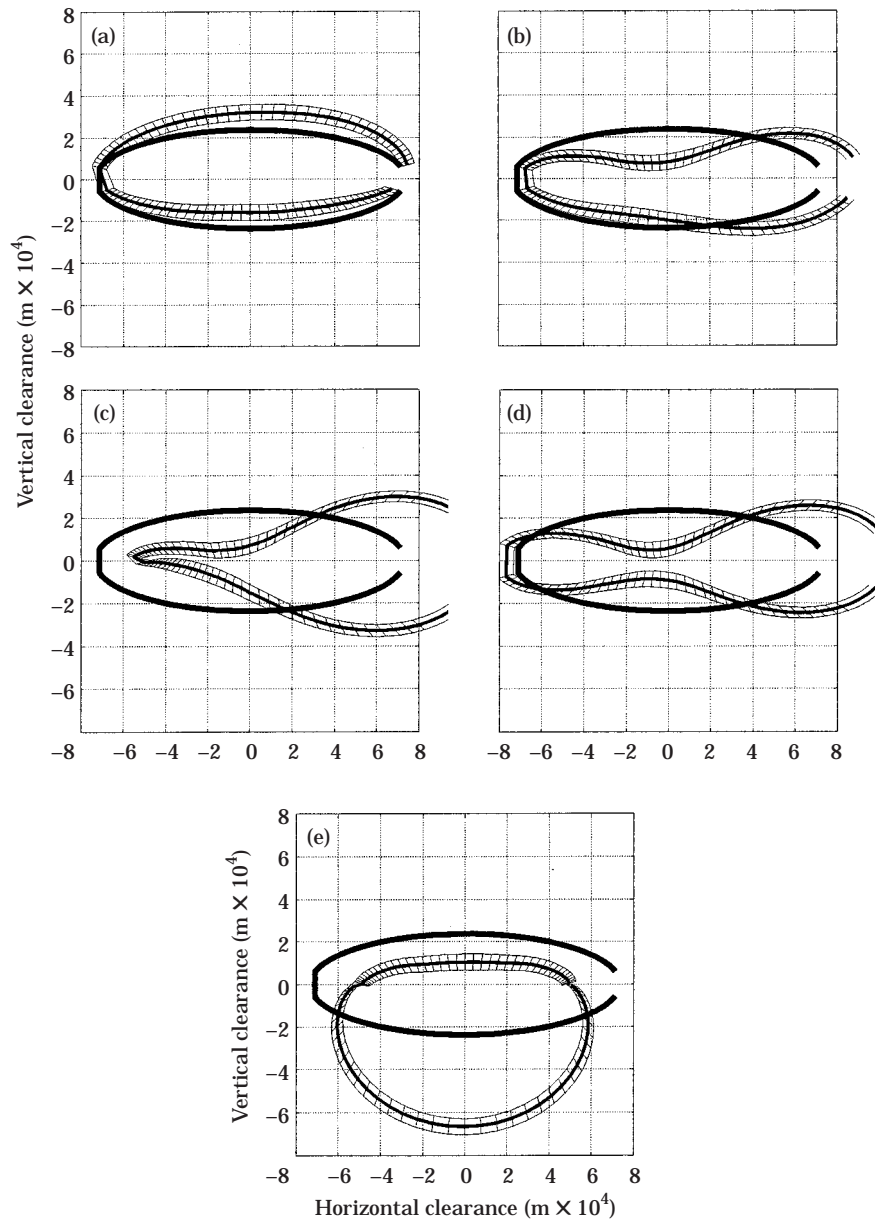
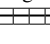


Figure 12. Shapes of the deformed clearance of bearing no. 6 for individual versions of initial clamping. (a) Without the initial clamping; (b) initial clamping as in Figure 11(a) (case 1); (c) initial clamping as in Figure 11(b) (case 2); (d) initial clamping as in Figure 11(c) (case 3); (e) initial clamping as in Figure 11(d) (case 4). —, Undeformed clearance; , "real" clearance with working tolerances, $n = 3000$ rpm.

the bearing supports, and the initial clamp of the bushings during their assembly, on the dynamic properties of the whole system. It is assumed that the analysis should be conducted with the inclusion of thermoelastic deformation in the bushings. The aim of this research is to define the effect of accidental assembly errors connected with bushing clamps in the pedestals, and also to estimate the possibilities of optimizing the method of setting the bush external fixings. There is no reliable information about this subject in the

literature. The KINWIR and NLDW computer programs enable this kind of analysis to be done owing to the complex, 3-D thermal model of the bearing nodes.

The simulation research was conducted for various cases of assembly and initial clamping of the bearing bushes (see Figure 11). The initial clamping caused deformation of the oil clearance; see Figure 12. Such a strong change in the shape of the oil clearance results in changes in the dynamic response of the system under the synchronous external restraint, see Figure 13. It appears that the configuration as in Figure 11(d) (case no. 4), is the most profitable for the operation of the whole system, and especially for bearing

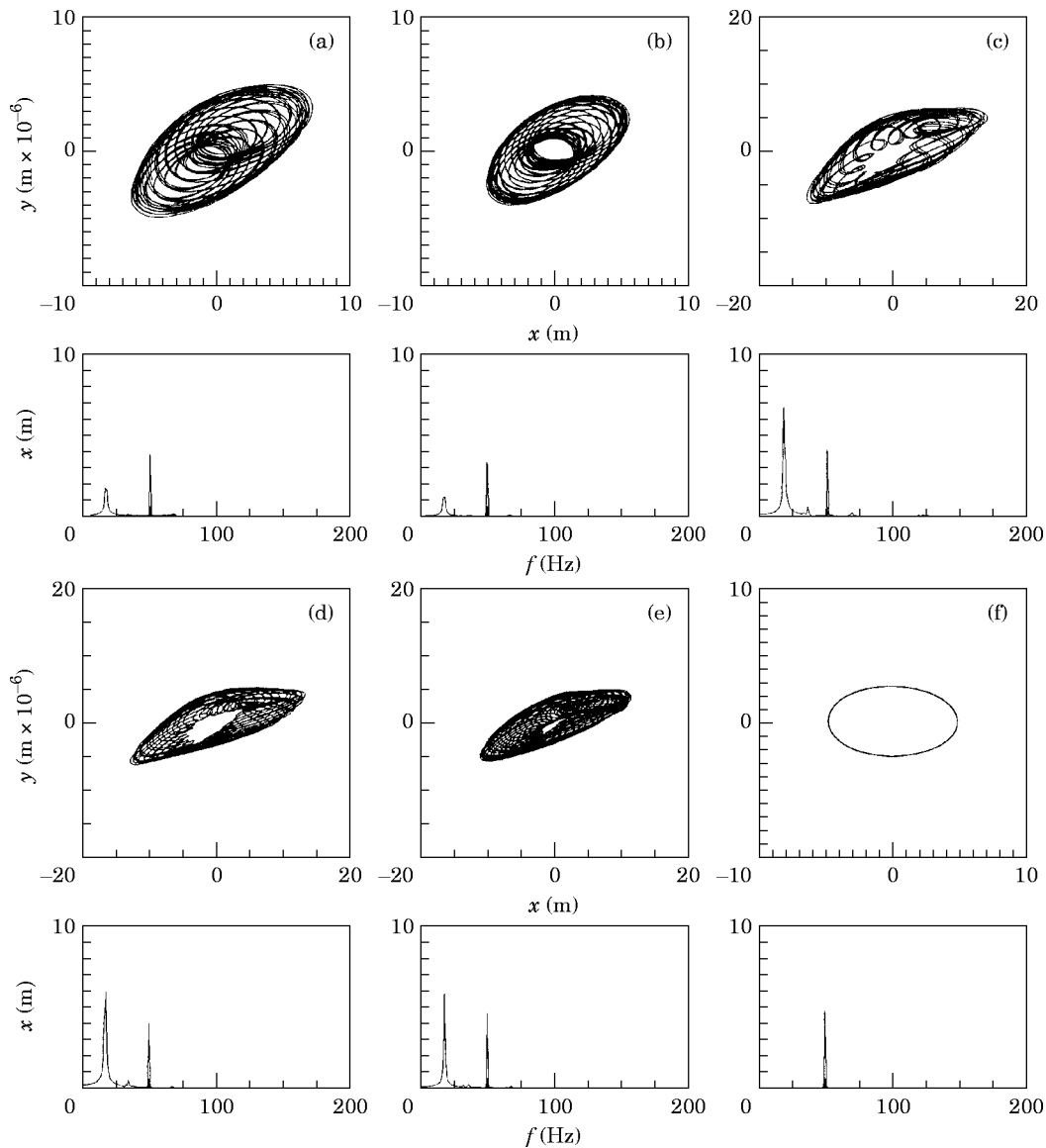


Figure 13. Trajectories and vibration spectra of bearing bush no. 6 in the horizontal plane during the excitation by a force of rotation ratio 1 n ; $n = 3000$ rpm. (a) The constructional clearance; (b) "real" clearance; (c) case 1; (d) case 2; (e) case 3; (f) case 4.

no. 6. It is characteristic that the effect of deformation of the oil clearance is relatively small under the external restraint of a frequency two times the rotational frequency.

The information obtained confirms the potential possibility of the optimization of the dynamic system properties by way of a suitable bearing bush assembly.

3.2. THE DYNAMICS OF THE LP CASING

In the analysis of the turbo-set dynamics, not only the information directly concerning the rotor and bearing lines, but also the remaining substructures, such as HP, IP and LP turbine casing characteristics, as well as those of the generator and the foundation can be of great importance. Here an example of the simulation research concerning the dynamics of perhaps the most complex of the mentioned substructures, i.e., the LP casing, is presented. In some large units, bearing supports are integrated with the construction of the LP casing. The information about the support stiffness coefficients can be obtained by analyzing the dynamics of the whole casing. Also the results concerning the resonance frequency of the casing, and changes in the support stiffness for different construction variants, can be significant. The calculation of the dynamics, applied together with the analysis of the dynamic reaction of the rotor lines and the bearings, offers interesting possibilities to build not only diagnostic relationships, but also to optimize the dynamic properties of the turbine/generator system by means of computer simulations.

The finite element method (FEM) and the ABAQUS system have been used in the calculations. In Figure 14 is shown an FEM mesh for the symmetric half of the LP casing of a large machine, the model having 60 000 degrees of freedom. The calculations of the excited vibrations of the casing have been carried out by using the method of modal analysis. In Figure 15 is shown an example of calculation results for vibration amplitudes and phase angles of bearing supports in the region of the casing for sinusoidal load functions operating at the same points for the rotational speed range $n = 300\text{--}3000$ rpm with the amplitude of 20 kN.

There is a large conspicuous difference between the vibration amplitudes of the bearings (especially for the vertical component), which can be easily explained by the assumed simplifications in FEM modelling. The differences in amplitude values for bearings no. 3 and 6 as well as no. 4 and 5 (see Figure 15) arise partly from the fact that the casing is

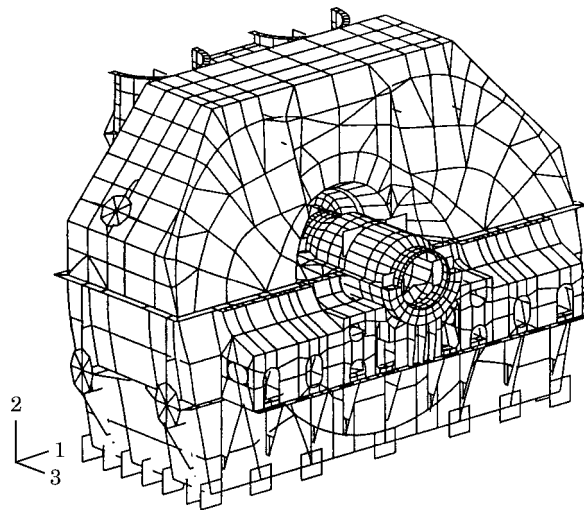


Figure 14. The FEM mesh for the symmetric half of LP casing (60 000 degrees of freedom).

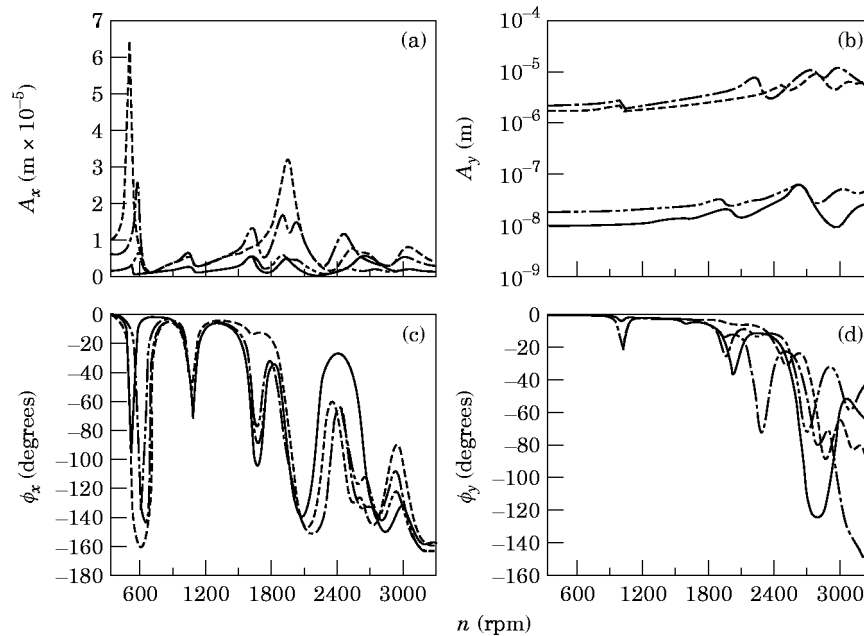


Figure 15. Horizontal (a, c) and vertical components (b, d) of vibration amplitudes and phase angles of bearing supports of the LP casing for an external sinusoidal excitation force applied to particular bearing supports. Bearing no.: - · - ·, 3; - - -, 4; ---, 5; —, 6.

non-symmetrically loaded. Amplitudes and phase angles directly influence the stiffness coefficients $\lambda_{i,k}$ and damping coefficients $A_{i,k}$ of the LP casing at the point of support of the bearing; see Figure 16, in which is presented a comparison of horizontal and vertical dynamic stiffness coefficients of bearing no. 5. It is interesting to note that the vertical dynamic stiffness coefficient is several times greater than the horizontal coefficient in the low frequency range (5–30 Hz). Moreover, it is very characteristic that an increase in

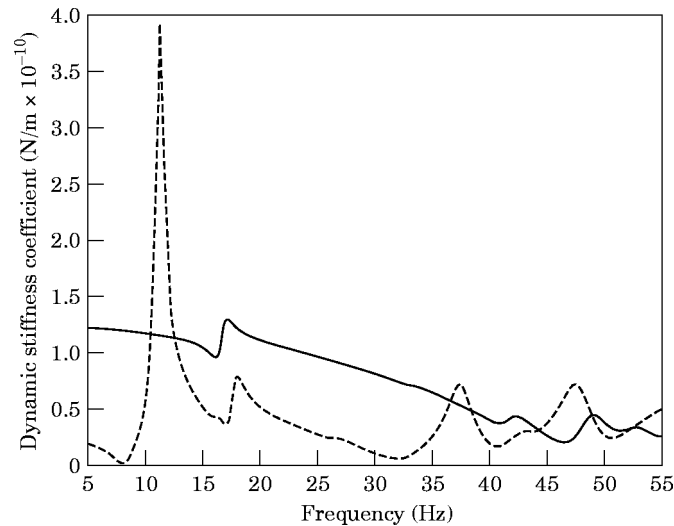


Figure 16. Dynamic stiffness coefficients of the LP casing at the point of support of the bearing no. 5: ---, c_{11} , horizontal component; —, c_{22} , vertical component.

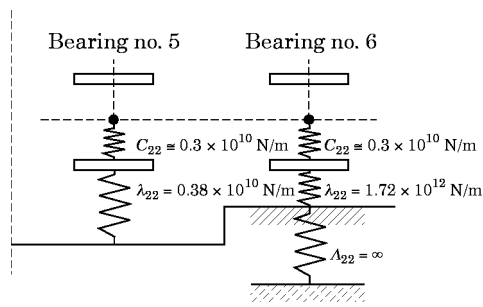


Figure 17. The comparison of elastic properties of the oil film c_{22} and bearing support λ_{22} at 50 Hz. c_{22} is the vertical component of the dynamic stiffness coefficient of the oil film and λ_{22} is the vertical component of the dynamic stiffness coefficient of the bearing support.

frequency indicates a continuous decrease in the vertical dynamic stiffness coefficient. The variation of the horizontal dynamic stiffness coefficient demonstrates resonance frequencies of the system—the most powerful being in the proximity of 8 and 32 Hz.

It is worth noticing that the dynamic stiffness coefficients $\lambda_{i,k}$ of the LP casing at the point of support of the bearing can reach similar or even smaller values than the dynamic stiffness coefficient of the oil film—the comparison is presented in Figure 17. Therefore, the bearing support can be equally important for the dynamic analysis of the turbo-set as the elastic and damping properties of the oil film.

The dynamic calculations of the rotors and bearings line for given values of $\lambda_{i,k}$ and $A_{i,k}$ were carried out with the help of the programs KINWIR and NLDW. These calculations provide valuable diagnostic relationships to assess different constructional configurations of the LP casing.

4. CONCLUSIONS

In the analysis presented of dynamic properties of a 200 MW turbo-set, we have concentrated on two basic topics. The first topic is the influence of thermoelastic deformation and initial clamp of the bearing bushes on the dynamic properties of the rotor line system. It is worth emphasizing that the non-linear model of the object analyzed is used here. The second subject is the analysis of the dynamic stiffness of the LP casing at the fixing points of the bearing bushes. The results obtained lead to the following conclusions.

1. The thermoelastic deformation of the bearing bushes can be decisive for the dynamic properties of the rotor system. In the cases of substantial changes in the oil clearance geometry caused by initial clamping forces or the fixing method of the bush external surfaces, the inclusion of thermoelastic deformations can essentially affect the obtained results of dynamic analysis of the system. As shown in the examples presented, the analysis of deformation of the bearing clearance can also be employed in the optimization of the dynamic properties of the system. However, it should be underlined that the thermoelastic deformation influences the picture of the vibrations of the system only under the action of synchronous forces such as those caused by an unbalance of the rotating mass. On the other hand, under the action of a force of a frequency two times the rotational frequency (for example the electromagnetic forces) this deformation does not cause changes in the level and distribution of vibration spectrum of the system.

2. The comparison of the results of the forced vibration analysis for the rotor line with cases of “actual clearance” and construction clearance does not show any essential

differences. Thus, the inclusion of thermoelastic deformation of the bearing clearance for the normal fixing conditions does not change the results of the dynamic analysis of the system.

3. The analysis of dynamic properties of the LP casing at the points of support of the rotor shows that the vertical dynamic stiffness in support no. 5 exhibits a decreasing tendency. During the operational frequency (about 50 Hz) its value is comparable with the stiffness of the lubricating film. This may disadvantageously affect the dynamic properties of the whole turbo-set.

4. The characteristics obtained of the dynamic stiffness of the supports investigated rule out the prior suggestion of the necessity of changing the dynamic properties of the construction by stiffening support no. 6. It appears that the stiffness of this support is already higher by two orders of magnitude than the stiffness of the support of bearing no. 5.

It should be stressed that the simulation research of dynamic states of real objects can be a very useful source of information in the process of acquiring diagnostic relationships. It refers especially to the extreme states of machine operation where experimental research is out of the question. A very important advantage of the simulative methods is the possibility of separating the effects of various factors and external forces. This is not always possible in non-simulative analysis, especially in the case of real objects of very complex structure of the vibration spectrum.

REFERENCES

1. J. DING, and M. KRÓDKIEWSKI 1993 *Journal of Sound and Vibration* **164**, 267–280. Inclusion of static indeterminacy in the mathematical model for non-linear dynamic analyses of multi-bearing rotor system.
2. H. HATORI and N. KAWASHIMA 1991 *Japan Society of Mechanical Engineers International Journal III* **34**(4), 503–511. Dynamic analysis of a rotor–journal bearing system with large dynamic loads.
3. M. M. KHONSARI and Y. J. CHANG 1993 *Transactions of the American Society of Mechanical Engineers, Journal of Vibration and Acoustics* **115**, 303–307. Stability boundary of non-linear orbits within clearance circle of journal bearings.
4. A. MUSZYŃSKA, W. D. FRANKLIN and D. E. BENTLY 1988 *Transactions of the American Society of Mechanical Engineers, Journal of Vibration, Acoustics, Stress and Reliability in Design* **110**(2), 143–150. Rotor active “anti-swirl” control.
5. V. PAVELIC and R. S. AMANO 1992 *Proceedings of the Turbo-Expo International Conference, Cologne*. A study of transient response of flexible rotors in high speed turbo-machinery.
6. M. RUSSO and R. RUSSO 1993 *Proceedings of the Institution of Mechanical Engineers, Part C: Journal of Mechanical Engineering Science* **207**, 149–160. Parametric excitation instability of a rigid unbalanced rotor in short turbulent journal bearings.
7. R. SUBBIAH and N. F. RIEGER 1988 *Transactions of the American Society of Mechanical Engineers, Journal of Vibration, Acoustics, Stress and Reliability in Design* **110**, 515–520. On the transient analysis of rotor–bearing systems.
8. M. L. ADAMS, M. L. ADAMS and J. S. GUO 1996 *IMEchE Conference Transactions, Vibrations in Rotating Machinery*, 309–319. Simulations and experiments of non-linear hysteresis loop for rotor–bearing instability.
9. J. KICIŃSKI 1994 *Teoria i badania hydrodynamicznych łożysk ślizgowych (Theory and Investigations of Journal Bearings)*. Wrocław: Ossolineum, first edition.
10. J. KICIŃSKI 1986 *Wear* **111**, 289–311. Influence of the flow prehistory in the cavitation zone on the dynamic characteristics of slide bearings.
11. J. KICIŃSKI 1989 *Wear* **132**, 205–220. New method of description of dynamic properties of slide bearings.
12. J. KICIŃSKI 1991 *Transactions of the Institute of Fluid-Flow Machinery* **93**, 163–194. The influence of thermoelastic deformation of bearing bush and its external fixings on static and dynamic properties of journal bearings, Parts I and II.

13. J. KICIŃSKI 1993 *Machine Dynamics Problems, Warsaw* **6**, 37–60. Influence of thermal phenomena in the slide bearings on the dynamics of a simple rotor–bearings system.
14. J. KICIŃSKI 1996 *Transactions of the Institute of Fluid-Flow Machinery, Gdańsk* **100**, Non-linear model of vibrations in rotor–bearings system, part I: calculation algorithm.

APPENDIX: NOMENCLATURE

$c_{i,k}$	stiffness coefficients of the oil film (N/m)	x, y	rectangular co-ordinates connected with the static equilibrium position of the bush (see Figure 1)
$d_{i,k}$	damping coefficients of the oil film (Ns/m)	z	coordinate along the bearing axis; the geodesic rotor co-ordinate
D	global matrix of damping (Ns/m)	g	centre line angle (rad)
e	eccentricity of the bearing (m)	μ	oil dynamic viscosity (Ns/m ²)
h	oil clearance thickness (m)	$\bar{\mu}$	oil mean “effective” viscosity (Ns/m ²)
K	global matrix of stiffness (N/m)	ξ, η	curvilinear coordinates—circumferential and across the oil film
M	global matrix of inertia (Ns ² /m)	ξ_1^*, ξ_2^*	co-ordinates defining the boundary of a continuous non-cavitating oil film
L	bearing width (m)	ψ	angular co-ordinate, $\psi = \xi/R$ (rad)
n	rotor rotational speed (rpm)	$\lambda_{11}, \lambda_{22}$	stiffness coefficients of the bush external fixings, horizontally and vertically (N/m)
$(O_p)_{st}, (O_c)_{st}$	position of static equilibrium of the bearing bush and journal	τ	$= \omega, t$, angle determining the position of the disc imbalance vector in relation to axis x (in degrees)
O_c	temporary position of the journal centre during dynamic loading	ω	rotor angular velocity (rad/s)
q	vector of displacements (m)		
P	vector of dynamic external forces of the system (N)		
p	hydrodynamic pressure in the oil film (N/m ²)		
r	radial co-ordinate (see Figure 1) (m)		
R	journal radius (m)		
ΔR	absolute radial clearance (m)		
t	time (s)		